

Analysis of Self-Potential Response beyond the Fixed Geometry Technique

Harry Mahardika

Kelompok Keahlian Fisika Bumi dan Sistem Kompleks, FMIPA, Institut Teknologi Bandung, Jl. Ganesha No. 10 Bandung 40132, Indonesia

Corresponding author: hmahardi@fi.itb.ac.id

Abstract. The self-potential (SP) method is one of the oldest geophysical methods that are still available for today's application. Since its early days SP data interpretation has been done qualitatively until the emerging of the fixed geometry analysis that was used to characterize the orientation and the electric-dipole properties of a mineral ore structure. Through the expansion of fundamental theories, computational methods, field-and-lab experiments in the last fifteen years, SP method has emerge from its low-class reputation to become more respectable. It became a complementary package alongside electric-resistivity tomography (ERT) for detecting groundwater flow in the subsurface, and extends to the hydrothermal flow in geothermal areas. As the analysis of SP data becomes more quantitative, its potential applications become more diverse. In this paper, we will show examples of our current SP studies such as the groundwater flow characterization inside a fault area. Lastly we will introduce the application of the "active" SP method - that is the seismoelectric method - which can be used for 4D real-time monitoring systems.

1. Introduction

Self-potential (SP) method corresponds to the passive measurements of electric signals associated with variety of source current mechanisms in the conductive subsurface of the earth. It is a geophysical method that everyone knows about but nobody seems to appreciate [1], hence it's named the ugly duckling of environmental geophysics. In the local scope, such as in the past HAGI annual meetings there are only few papers on SP method: one is applied in hydrothermal system study [2] and two are focusing in groundwater flow in porous media [3, 4]. In SP data analysis, there are two known methods of quantitative analysis (inversion) of SP data: 1. fixed geometry technique, and 2. continuous model inversion. The fixed geometry inversion is based on the solution of Poisson equation for electrical problem that is created from electrically-polarized structures (electrical dipole) along a principal profile over the body [5]. Here, the physical mechanism that is creating the electrical dipole however is not taken into account in the Poisson equation. On the other hand, the continuous model inversion is based on the solution of Poisson equation that is generated from either redox-based contribution [6, 7] and streaming current contribution related to groundwater flow [7]. The two inversion methods were applied for various near surface applications where the former are relatively more widely used for SP studies in Indonesia due to its simplicity and effectiveness in terms of computation time [8, 9]. Therefore, we present our current research on continuous model inversion for SP data by doing a quick review on the fixed geometry technique and its limitation, and then



describing the formulation of continuous model inversion with application example, and introducing the time-lapse expansion of SP inversion with prospect application in water encroachment monitoring.

2. SP and Fixed Geometry Inversion

The fixed boundary inversion for electric potential formulation is based on a polarized structure along a principal profile over an ore body [10]. Considering a polarized body located at the 2D homogeneous medium and its polarization axis pointing towards geographical North direction we will have an electric potential described at an observation point:

$$\varphi(x, z, K, \theta) = K \frac{(x - x_s) \cos \theta + (z - z_s) \sin \theta}{\left[(x - x_s)^2 + (z - z_s)^2 \right]^q} \quad (1)$$

where K is an electric dipole moment (in mV), θ is the dipole orientation from positive vertical axis, and (x_s, z_s) are the horizontal and vertical dipole source location (in m). In this formulation, geometrical factor q is a quantity related to the shape of the anomaly such as sphere ($q = 1.5$), horizontal cylinder ($q = 1$), and vertical cylinder ($q = 0.5$). Given a specific geometrical factor that we want to recover, we estimate four quantities that is shaping the model vector $\mathbf{m} = [x_s, z_s, K, \theta]$.

The application of the fixed geometry technique is presented in the following example where real SP data was collected from the Intra-Mural Field of Colorado School of Mines, shown in figure 1a. In this case, a preliminary SP surface map is obtained and we chose SP profile line A-B for inverse calculation. Applying initial guess of $(x_s, z_s, K, \theta) = (0 \text{ m}, -10 \text{ m}, 10 \text{ mV}, 45^\circ)$ and fix the geometrical factor $q = 0.5$ representing a vertical cylinder structure, we get a good fit of SP field response with the inverse calculation after 333 iterations as it shown in figure 1b. The inverse calculation, done using Gauss-Newton technique, is also recover the structure location in $x_s = 15 \text{ m}$ and $z_s = -24 \text{ m}$ and the electric dipole parameters $K = -14.5 \text{ mV}$, and $\theta = 73^\circ$. The inversion result shows differences with the previous interpretation of the data, which suspect that the location of a buried pipe is 12 m further from the current estimation (grey boxes at figure 1a).

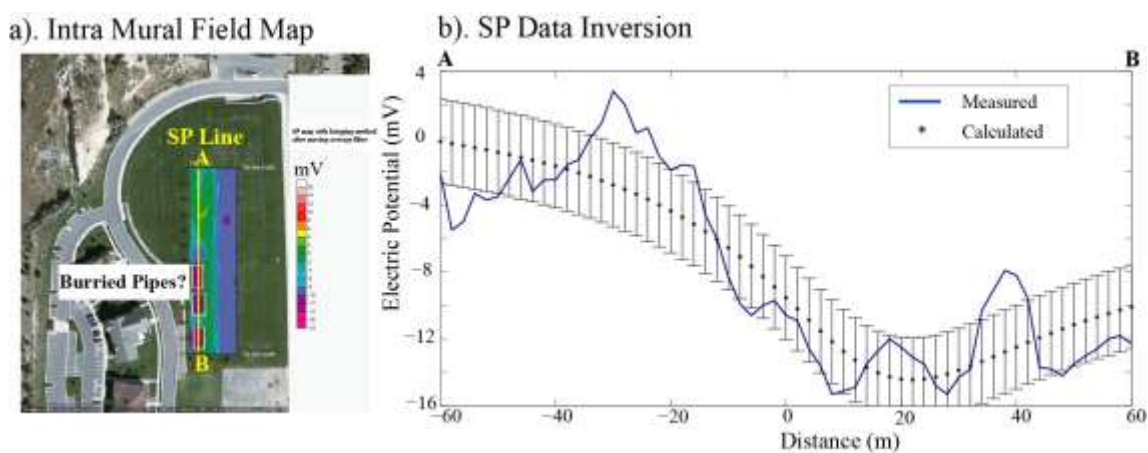


Figure 1. Intra Mural SP example. As it shows here, a). is the location of Intra Mural Field, CSM, where surface SP measurements conducted and profile line A-B was selected. And in b). is showing SP data along profile A-B and the inverse calculation result showing a fairly good agreement between them

There are several variations that can be done for fixed geometry technique application. Candra et.al [9] shows the usage of singular value decomposition technique for finding the inverse solution of several synthetic and measured SP test cases that is similar to the Intra Mural example. Other example [11] expands the formulation of equation 1 such that it representing inclined sheet geometry of infinite horizontal extent to mimics the surface of a fault. In one example they reconstruct the center location and the dimension of the fault as well as the dipole density and its inclination angle. From these example however, it is clear that the fixed-geometry inversion of SP data with its entire variant is relatively limited in characterizing of the electric dipole and its position and orientation in the subsurface, and therefore could not be used for interpreting physical processes that really happen there. And this is where the continuous model approach plays a bigger role in the game.

3. Continuous Model Inversion for SP Data Analysis

The concept of continuous model inversion of SP response is based on the solution of electric Poisson equation that is generated from either redox-based contribution and streaming current contribution related to groundwater flow [7]

$$\nabla \cdot \sigma \nabla \varphi = \nabla \cdot \left[{}^{(1)} -\sigma \nabla E_H - {}^{(2)} \frac{1}{e} (\sigma_{(+)} - \sigma_{(-)}) \nabla \mu_f + {}^{(3)} Q_v \mathbf{u} \right] \quad (2)$$

where σ is the conductivity of porous medium whereas $\sigma_{(+)}$ and $\sigma_{(-)}$ are the conductivities of anions and cations respectively (all in S/m), μ_f is the electrochemical potential of pore fluid (in V), E_H is the redox potential (in V), and \mathbf{u} is the fluid flow or Darcy velocity [m/s]. The first term in the right hand side of the eq (2) is related to the physics of redox potential created in an ore body due to the presence of water table. The second one is related to the gradient of the chemical potential of the pore water solution (e.g., associated with a gradient of salinity or ionic strength) and the third is related to the flow of the pore water. These contribution are also called the diffusion current density and streaming current density respectively. The excess of charge Q_v (in C/m³) is controlling the electrokinetic process and related to the saturated permeability k_0 of the porous medium via an empirical relation [12] given

$$\log(Q_v) = -9.23494 - 0.8219 \log(k_0) \quad (3)$$

For simplicity, we can focus on the electrical signals of electrokinetic nature that are due to the streaming current density. We consider an isotropic but possibly heterogeneous medium such that the governing equation for the electrical problem [13] is given as

$$\nabla \cdot \sigma \nabla \varphi = \mathfrak{I} \quad (4)$$

where equation (4) is basically a Poisson's equation for the self-potential problem φ (expressed in V), and $\mathfrak{I} = \nabla \cdot (Q_v \mathbf{u})$ denotes the (scalar) volumetric current density (in A/m³). Therefore, the electric potential distribution at an observation points along the surface is given by

$$\varphi(x, y, z) = \int_V \mathbf{K}(x, y, z, x_s, y_s, z_s) \mathfrak{I}(x_s, y_s, z_s) dV \quad (5)$$

where $\mathbf{K}(x, y, z, x_s, y_s, z_s)$ is the kernel and dV is a small volume around the source point $\mathfrak{I}(x_s, y_s, z_s)$.

The continuous model technique formulated from equations (4 and 5) implies the importance of resistivity data in the inverse-model calculation. In most applications, resistivity information of the subsurface is given by the electrical dc-resistivity measurement or electromagnetic methods done in active or massive mode. From equation (5), the elements of the kernel are the Green functions connecting the self-potential data at a set of measurement stations located at the surface and the sources of current density located in the conducting volume. The kernel computation accounts for the electric resistivity distribution and the boundary conditions applied to the system. Therefore, the data are defined using 3D coordinates (x, y, z) , hence equation (5) can be written as

$$\mathbf{d} = \mathbf{K}\mathbf{m} \quad (6)$$

where \mathbf{m} is a model vector containing the M -source current density terms \mathfrak{J} , and \mathbf{d} denote the data vector of electric potentials φ observed in N -receiver locations. Subsurface model \mathbf{m} is expressed as $\mathbf{m} = [\mathbf{m}_1, \dots, \mathbf{m}_M]^T$ where \mathbf{m}_i , $i = 1, 2, \dots, M$; while the data vector \mathbf{d} is also written in the form of $\mathbf{d} = [\mathbf{d}_1, \dots, \mathbf{d}_N]^T$. The data misfit vector is defined in the spatial domain by

$$\mathbf{e} = \mathbf{K}\mathbf{m} - \mathbf{d} \quad (7)$$

In equation (7), forward modeling response $\mathbf{K}\mathbf{m}$ is specified for the electrical problem where kernel matrix \mathbf{K} is related to the analytical Green's function of the electric Poisson equation shown in equation (5). Using the least square solution of the misfit we construct an objective function ψ [13] that can be expressed as

$$\psi = \mathbf{W}_d \|\mathbf{G}\mathbf{m} - \mathbf{d}\|^2 + \alpha \|\mathbf{m}\|^2 \quad (8)$$

where \mathbf{W}_d correspond to the data weighting matrix, $\|\cdot\|^2$ denotes the L-2 norm, α is the (spatial) regularization parameter and \mathbf{G} is the Green's matrix computed from $\mathbf{G} = \mathbf{P}\mathbf{K}^+$ as a product of the inverse kernel matrix times the sparse selector matrix $\tilde{\mathbf{P}}$ that contains value of 1 on each row in the column that correspond to the location of the receivers.

The least square solution of equation (8) is now applied for analysis of an SP data collected at the Pinggirsari county, Banjara, of the Bandung Regency. The goals of the survey are to identify the subsurface fault location and orientation, as well as to characterize the geologic strata over the area. In this study we conduct not only SP but also dc resistivity (or electric resistivity tomography / ERT) that we use for SP inversion input. In that sense, the SP data and the resistivity data are collected in the same profile line along the Pinggirsari - Majalaya county road. The result of the resistivity measurements is shown in the tomogram of figure 2a where possible existence of a fault on the subsurface is observed. In figure 2b we show the good fit of the inverse calculated electrical response (presented in black dots with error bars) and measured SP data (presented in blue line). Whereas in figure 2c we show the reconstructed volumetric current density that shows a dipole-like anomaly on the edge of the possible fault, with stronger positive magnitude. This could show the existence of possible groundwater flow along the fault plane from top to bottom direction. Another dipolar anomaly on the top middle-right of current density section will be analyzed for later study, but possibly not related to groundwater flow but rather electrochemical one.

4. The Future is Time-Lapsed Inversion?

The expansion of SP analysis from fixed geometry into continuous model inversion is necessary due to the SP inverse problem is similar in essence to electroencephalography (EEG) in medical imaging.

In this case, the subsurface is defined as a space-time model, which encompasses all space models during the entire monitoring periods. So now, the entire monitoring data are defined using 3D coordinates (x, z, t) . In this case, subsurface model $\tilde{\mathbf{m}}$ is sparsely sampled at some pre-selected times and is expressed as $\tilde{\mathbf{m}} = [\mathbf{m}_1, \dots, \mathbf{m}_t]^T$ where \mathbf{m}_i , $i = 1, 2, \dots, t$ is the model for the i -th time step and t is the number of monitoring times. The data misfit vector is defined in the space-time domain by

$$\mathbf{e} = \tilde{\mathbf{K}}\tilde{\mathbf{m}} - \tilde{\mathbf{d}} \quad (9)$$

In eq (10), the vector $\tilde{\mathbf{d}}$ corresponds to the electrical data vector defined in the spatial coordinate system by $\tilde{\mathbf{d}} = [\mathbf{d}_1, \dots, \mathbf{d}_t]^T$. Forward modeling response $\tilde{\mathbf{K}}\tilde{\mathbf{m}}$ is specified for the electrical problem where kernel matrix $\tilde{\mathbf{K}}$ is related to the analytical Green's function of the electric Poisson equation.

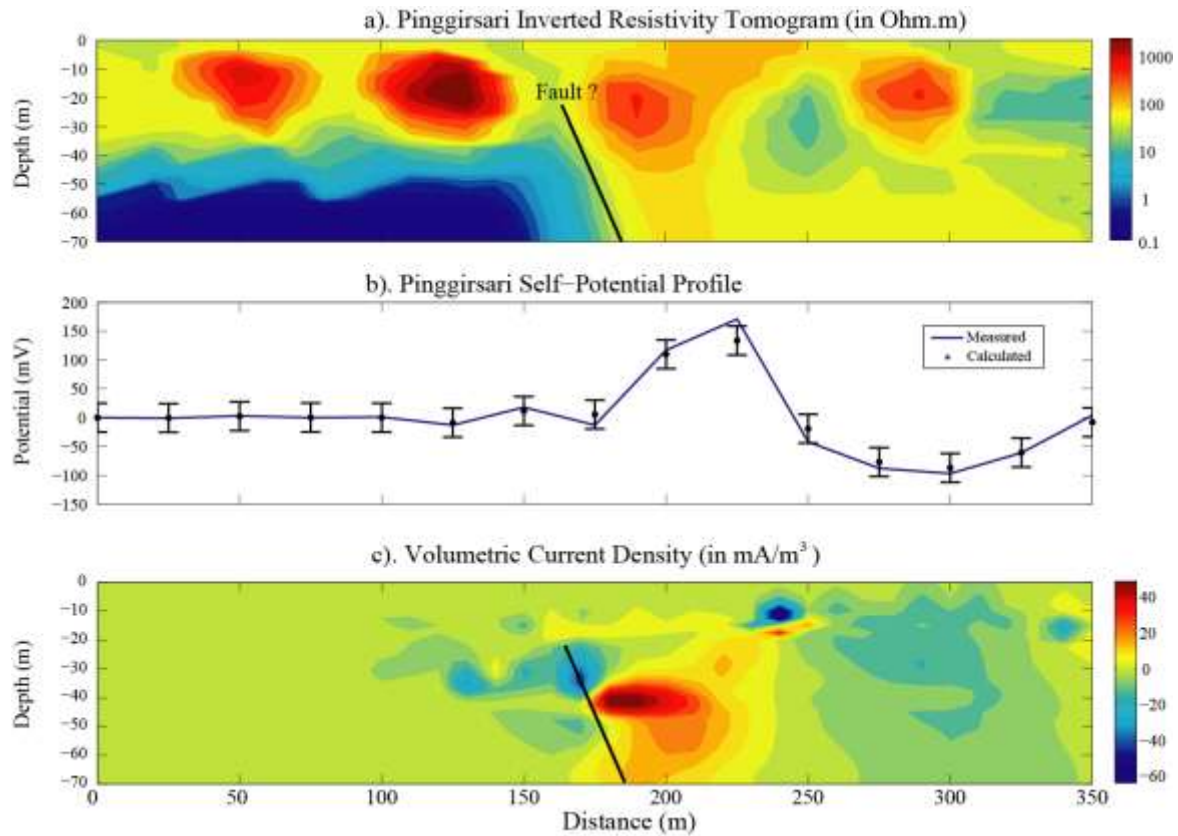


Figure 2. Results from Pinggirsari Survey. a). The resistivity tomogram shows possible existence of a fault on the subsurface. b). The inverse calculation of the electrical response (black dots) is in a good fit with the measured SP data (blue line). c). The reconstructed volumetric current density show dipole like anomaly on the edge of the possible fault.

The solution of eq (10) is computed with some modification of the 4D-ATC algorithm such that it will adopt two regularizations in space and time domains to stabilize the inversion calculation. The objective function $\Psi_{\tilde{\mathbf{m}}}$ [14, 15] can be expressed as

$$\Psi_{\tilde{\mathbf{m}}} = \mathbf{W}_d \|\tilde{\mathbf{G}}\tilde{\mathbf{m}} - \tilde{\mathbf{d}}\|^2 + \alpha \|\tilde{\mathbf{m}}\|^2 + \gamma \|\tilde{\mathbf{P}}\|^2 \quad (10)$$

where \mathbf{W}_d correspond to the data weighting matrix, $\|\cdot\|$ denotes the L-2 norm, α is the (spatial) regularization parameter, Σ is a smoothness function for the time variation, γ is the time regularization parameters, and $\tilde{\mathbf{G}}$ is the Green's matrix computed from $\tilde{\mathbf{G}} = \mathbf{P}\tilde{\mathbf{K}}^{-1}$ as a product of the inverse kernel matrix times the sparse selector matrix $\tilde{\mathbf{P}}$ that contains value of 1 on each row in the column that correspond to the location of the receivers.

Inverted Volumetric Current Density (in $\mu\text{A}/\text{m}^3$) using Time-Lapse Weighted Least Square

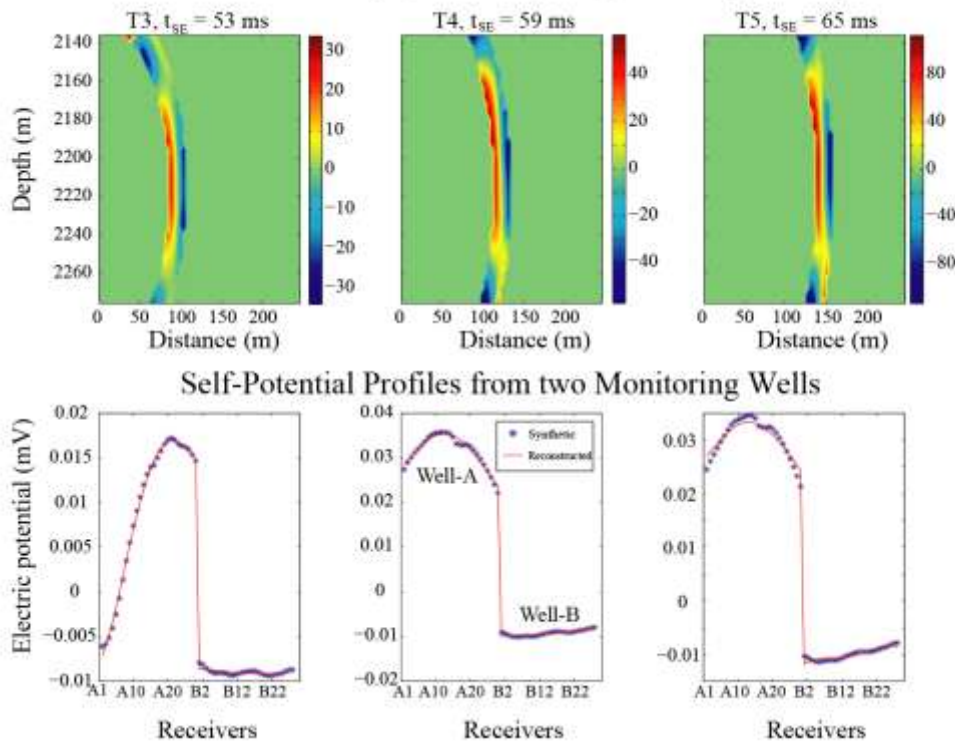


Figure 3. The inverted volumetric current densities of seismoelectric signals at any given arrival times for each saturation profiles ($t_{SE} = 53$ ms from saturation profile T3, $t_{SE} = 59$ ms from saturation profile T4, and $t_{SE} = 65$ ms from profile T5).

To illustrate the usefulness of time lapse inversion for SP response we use one example from water encroachment problem given in Revil and Mahardika (2013) [16]. Here, we use seismoelectric method which describes the generation of electrical and electromagnetic disturbances associated with the occurrence of seismic sources and seismic wave propagation in partially or totally water-saturated porous media. In other word, it is the active version of the typical SP method that we know. The author wish the reader to look at the given reference [16] for further details on the geometrical setting of the study, the process of the flooding monitoring, and the picking of the saturation profiles. In this problem, the volumetric current density (taken from the seismoelectric response due to water saturation contrast) calculated using the time independent least square solution did not give a satisfactory inversion result. So, we apply time constraining factor computed from the average radiuses of the wavefronts from saturation profiles T3 to T5. Using this adaptive function we get a new inversion result shown in figure 3. In the top half of figure 3 we show the inverted volumetric current densities concentration which all of the current densities are located at the weighted region or close to the waterfront boundary. Here, the dipolar shape-like current density solution is physically realistic due to seismoelectric effect is created from imbalance of charge distribution across the saturation contrast that induced electrical current via electrokinetic effect [17, 18]. While in the bottom

half of figure 3 we show the computed electrical response is fairly in a good fit with the synthetic data taken from Well-A and Well-B.

5. Conclusion

In this paper we have shown examples of our current SP studies, one is the characterization of groundwater flow along a possible fault surface and another is the synthetic real time monitoring of fluid injection experiment. Through the expansion of fundamental theory, computational methods, and field-and-lab experiments in the last fifteen years, SP method has become a complementary package alongside electric-resistivity tomography (ERT) for detecting fluid flow for hydrological application, which also extends to the hydrothermal flow in geothermal areas [19]. As the analysis of SP data becomes more quantitative its potential applications becomes more diverse. Analysis of SP data should not done only with fixed geometry technique, but it have to expand to continuous model inversion due to its similarity to electroencephalography (EEG) in medical imaging. In the last decade, the recording and inversion of EEG signals has been instrumental in our understanding of how the brain works and in the mapping of its various functions. Therefore we can apply this technique in hydrology and geoscience in general in order to get similar purposes as EEG in neuroscience.

Acknowledgements

The author thanks the head of KK Fisika Bumi dan Sistem Kompleks Prof. Doddy Sutarno for his support on the project, Head of the Lab Permodelan dan Inversi EM Dr. Wahyu Srigutomo for his permission on using the data and the members of the Banjaran field-team for their collaboration on the project.

References

- [1] J.E. Nyquist and C. E. Corry, *The Leading Edge* 21, pp. 446–451(2002).
- [2] W. Srigutomo, A. S. Sunarya, C. M. Sufyana, A. Singarimbun, P. M. Pratomo, and E. C. Novana, “Pemodelan Self-Potensial untuk Investigasi Sistem Hidrotermal Dangkal Kawah Domas Gunung Tangkuban Parahu Bandung Jawa Barat,” in *Prosiding PIT HAGI 2009*.
- [3] M. H. Syahrudin, “Detecting Groundwater Flow In Porous Media Feeding Into A Nearby Spring,” in *Prosiding PIT HAGI 2010*.
- [4] M. Hamzah, D. Santoso, W. Parnadi, “Self-Potential Study For Laboratory Measurements Of Electrokinetic Potentetial From Fluid Flow In Porous Media,” in *Prosiding PIT HAGI 2007*.
- [5] S. Yungul, *Geophys.* 15, 237-246 (1950).
- [6] M. Sato and H. M. Mooney, *Geophys.* 25, 226–249 (1960).
- [7] A. Revil and A. Jardani, *The Self-Potential Method Theory And Applications In Environmental Geophysics* (CUP, Cambridge, 2013), pp. 23-77
- [8] W. Srigutomo, E. Agustine, and M. H. Zen, *Indones. J. Phys.* 17, 49–55 (2006).
- [9] A. D. Candra, W. Srigutomo, and B. J. Santosa, “A Complete Quantitative Analysis of Self-Potential Anomaly Using Singular Value Decomposition Algorithm,” in *Proc. of the IEEE Int. Conf. on Smart Instr., Meas. and Appl. (ICSIMA)*, DOI: 10.1109/ICSIMA.2014.7047419
- [10] B. B. Bhattacharya, and N. Roy, *Geophys. Prosp.* 29, 102-107 (1981).
- [11] S.P. Sharma and A. Biswas, *Geophys.* 78, WB3–WB15 (2013).
- [12] A. Jardani, A. Revil, A. Boleve, *Geophys. Res. Letters* 34, L24403 (2007).
- [13] B. J. Minsley, J. Sogade, and F. D. Morgan, *J. Geophys. Res.* 112, B02202 (2007).
- [14] Y. Zhang, A. Ghodrati, and D.H. Brooks, *Inv. Prob.* 21, 357–382 (2005).
- [15] J. H. Kim, M.J. Yi, S.G. Park, and J.G. Kim, *J. Appl. Geophys.* 68, 522-532 (2009).
- [16] A. Revil and H. Mahardika, *Water Resour. Res.* 49, 744–766 (2013).
- [17] Haartsen, M.W. and S. Pride, *J. Geophys. Res.* 102, 24745–24769 (1997).
- [18] Haines, S., “Seismoelectric imaging of shallow targets”, PhD. dissertation, Stanford Univ, 2004.
- [19] A. Revil and A. Jardani, *The Self-Potential Method Theory And Applications In Environmental Geophysics* (CUP, Cambridge, 2013), pp. 192-282.